


Influence of pulsed and continuous substrate inputs on freshwater bacterial community composition and functioning in bioreactors

Monica Ricão Canelhas,[‡] Martin Andersson,[‡]
Alexander Eiler,[†] Eva S. Lindström  and
Stefan Bertilsson*

¹Department of Ecology and Genetics/Limnology,
Uppsala University, Norbyvägen 18D, Uppsala, 752 36,
Sweden.

Summary

Aquatic environments are typically not homogenous, but characterized by changing substrate concentration gradients and nutrient patches. This heterogeneity in substrate availability creates a multitude of niches allowing bacteria with different substrate utilization strategies to hypothetically coexist even when competing for the same substrate. To study the impact of heterogeneous distribution of organic substrates on bacterioplankton, bioreactors with freshwater bacterial communities were fed artificial freshwater medium with acetate supplied either continuously or in pulses. After a month-long incubation, bacterial biomass and community-level substrate uptake rates were twice as high in the pulsed treatment compared to the continuously fed reactors even if the same total amount of acetate was supplied to both treatments. The composition of the bacterial communities emerging in the two treatments differed significantly with specific taxa overrepresented in the respective treatments. The higher estimated growth yield in cultures that received pulsed substrate inputs, imply that such conditions enable bacteria to use resources more efficiently for biomass production. This finding agrees with established concepts of basal maintenance energy requirements and high energetic costs to assimilate substrates at low concentration. Our results further imply that degradation of organic matter is influenced

by temporal and spatial heterogeneity in substrate availability.

Introduction

Substrate quantity and quality as well as the availability of inorganic nutrients are important regulators of bacterial growth and growth efficiency (Vallino *et al.*, 1996; del Giorgio and Cole, 1998). Bacterial communities are known to react strongly to changes in substrate supply (Tranvik, 1988; Grover and Chrzanowski, 2000; Pernthaler *et al.*, 2001) and individual populations also display preferences and variable affinities for specific substrates (Beier and Bertilsson, 2011; Salcher *et al.*, 2013). Accordingly, substrate composition and availability can be strong selective forces in shaping the composition of bacterial communities (Eiler *et al.*, 2003; Langenheder *et al.*, 2005; Judd *et al.*, 2006; Landa *et al.*, 2014). While some populations adapt to low concentrations by high affinity uptake systems (Salcher *et al.*, 2011) other bacteria will adopt an opportunistic life strategy and rapidly grow to higher abundances when substrates become plentiful (Salcher *et al.*, 2013). Patchiness in substrate availability over time and space may therefore enable a diverse set of seemingly functionally redundant heterotrophic organisms to coexist in the ecosystem (Salcher *et al.*, 2013) offering an explanation to how metabolically similar species can avoid competitive exclusion (Hutchinson, 1961).

A few studies have described bacterial exploitation of substrate patches in aquatic ecosystems (Blackburn *et al.*, 1998; Stocker *et al.*, 2008; Stocker, 2012) and the genomic underpinning of substrate acquisition strategies (Lauro *et al.*, 2009). Studies specifically addressing how substrate delivery rate and concentration influence bacterial community composition are few, and have mainly been based on modelling approaches (Konopka *et al.*, 2002; Lennon and Cottingham, 2008; Eichinger *et al.*, 2009). It has been suggested that members of communities continuously receiving low substrate inputs are expected to uphold cellular maintenance also under starvation and this would in theory result in lower growth yield compared to populations

Received 27 May, 2016; revised 17 October, 2017; accepted 30 October, 2017. *For correspondence. E-mail stebe@ebc.uu.se; Tel. +46 18 4712712; Fax +46 18 4712000. [†]Present address: eDNA solutions Ltd, Björkåsgatan 16, Mölndal, 43131, Sweden [‡]Both authors contributed equally to this work.

exploiting transient pulses of higher substrate availability (del Giorgio and Cole, 1998; Konopka, 2000).

Inspired by previous experiments (Carrero-Colón *et al.*, 2006; Konopka *et al.*, 2007), we hypothesized that continuous and pulsed supply of acetate would select for bacterial communities with different community composition. Specifically, we expected a community exposed to pulses of acetate to feature higher diversity due to temporal heterogeneity in resource supply, creating multiple niches (van Gemerden, 1974). Additionally, we further hypothesized that a continuously low concentration of acetate would lead to a more specialized community, favouring taxa with higher affinity towards acetate uptake and that substrates delivered in this way would be used at lower growth efficiency.

We investigated the effects of variation in substrate delivery by comparing continuously fed bioreactors to treatments receiving pulsed organic substrate inputs. An experiment was conducted with acetate as single carbon source and with total carbon concentrations representative for an oligotrophic freshwater lake ecosystem. During a month-long incubation, lake bacterioplankton communities in both treatments were supplemented with an equal amount of acetate as either pulsed additions or provided continuously. Acetate was chosen as substrate as it represents a dominant low molecular weight substrate for freshwater bacterioplankton, being produced both from photochemical degradation of humic substances (Bertilsson and Tranvik, 1998) and excretion from actively photosynthesizing phytoplankton (Bertilsson and Jones, 2003) while also accumulating as metabolic intermediates under anoxic conditions (Lovley and Klug, 1982).

Results

Bacterial growth yield

At the start of the experiment, the mean bacterial cell abundance was not significantly different between the two treatments (*t*-test, *p*-value = 0.32) with $1.54 \times 10^6 \pm 5.58 \times 10^5$ cells ml^{-1} ($n = 6$) in the pulsed treatment and $1.25 \times 10^6 \pm 4.18 \times 10^5$ cells ml^{-1} ($n = 6$) in the continuous treatment. During the experimental incubations, the abundance became approximately twice as high in the pulsed treatment with final abundances after one month of incubation at $1.72 \times 10^6 \pm 4.95 \times 10^5$ cells mL^{-1} in the pulsed treatment and $9.23 \times 10^5 \pm 4.80 \times 10^5$ ($n = 6$) cells ml^{-1} in the continuous treatment (Fig. 1). There was a significant difference in abundance between the two treatments throughout the incubation period (within-subjects ANOVA, $F(28,232)$, 2.94, *p*-value < 0.001), with the first significant difference observed already after the second pulse, on day 6 of the incubation (*p* < 0.001). The average acetate concentration in the reactor feed was $220 \mu\text{g C L}^{-1}$ for both treatments while the analytically determined standing stock

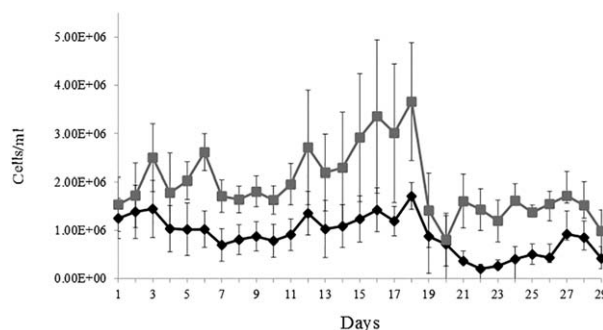


Fig. 1. Bacterial abundance over time in the continuous (black) and pulse (grey) substrate delivery treatments. Each data point represents averages of the treatments ($n = 6$) with error bars for standard deviation.

of acetate in the reactors just before the acetate uptake assays at the end of the month-long experiment was equal for both treatments (13 ± 3.1 and $13 \pm 4.0 \mu\text{g C L}^{-1}$ for the continuous and pulsed reactors respectively). Similar acetate levels ($13 \pm 2.7 \mu\text{g C L}^{-1}$) were seen in Milli-Q water blanks subjected to membrane filtration in the same way as the samples, suggesting that all of the added acetate was being used up in the reactors. Additionally, there was no significant difference in forward scatter (FSC) as a proxy for cell size between treatments (repeated measures ANOVA, $F[1,70]$, 0.047, *p*-value = 0.83; Supporting Information Fig. S1), suggesting that cell counts can be used to approximate differences in growth yield when comparing the two treatments.

Acetate degradation and uptake

At the end of the experiment, acetate degradation was monitored using HPLC following a $220 \mu\text{g C L}^{-1}$ acetate spike-in addition. Acetate decreased in all reactors, but degradation was more rapid in the pulse-fed reactors with no acetate remaining after 8 hours. In contrast, acetate remained at detectable concentrations in the continuously fed reactors even after 12 h of incubation (Fig. 2). Estimated acetate degradation rates were significantly different between treatments (*t*-test, *p*-value = 0.037) with average rates of $7.8 \pm 3.5 \mu\text{g C L}^{-1} \text{h}^{-1}$ for the continuously acetate fed communities and $22.5 \pm 11.8 \mu\text{g C L}^{-1} \text{h}^{-1}$ for the pulse-fed communities. After normalization for cell abundances, there were no significant differences in cell specific uptake rates between the two treatments (*t*-test, *p*-value = 0.11).

In the ^{14}C tracer addition experiments, labelled acetate was added to the reactors at $17 \mu\text{g C L}^{-1}$, substantially lower than the previously described acetate spike-in experiments. Assuming negligible in situ acetate concentrations, estimated total acetate assimilation rates were on average $0.23 \pm 0.03 \mu\text{g C L}^{-1} \text{h}^{-1}$ and $0.55 \pm 0.19 \mu\text{g C}$

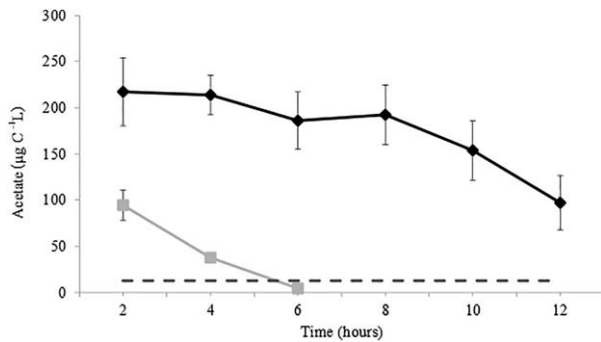


Fig. 2. Decrease of acetate concentration in reactors receiving continuous (black) and pulsed (grey) substrate delivery 2 h after spiking. Background (dashed line) indicates measured acetate concentrations in the reactor prior to the spike-in uptake experiments. The same concentration ($13 \mu\text{g C L}^{-1}$) was seen in filter blanks, suggesting that actual *in situ* acetate concentrations were negligible.

$\text{L}^{-1} \text{h}^{-1}$ for the continuous and pulsed treatments respectively and were significantly different between the treatments (*t*-test, *p*-value < 0.001; Supporting Information Table S7 for details). The lower acetate uptake rates compared to estimated degradation is likely due to high mineralization of the substrates being used, but may in part also result from contrasting substrate levels in the two assays. Similarly to the acetate spike-in degradation experiments, there were no significant differences in cell-normalized acetate processing rates between the treatments (*t*-test, *p*-value = 0.26), suggesting that the higher acetate processing capacity in the reactors receiving

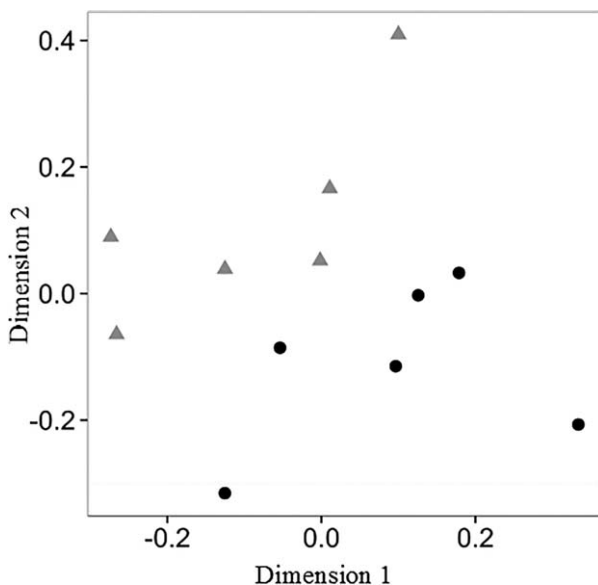


Fig. 3. NMDS plot of the bacterial communities in the continuous (filled circles) and pulsed substrate delivery treatments (grey triangle). Stress-value: 0.10.

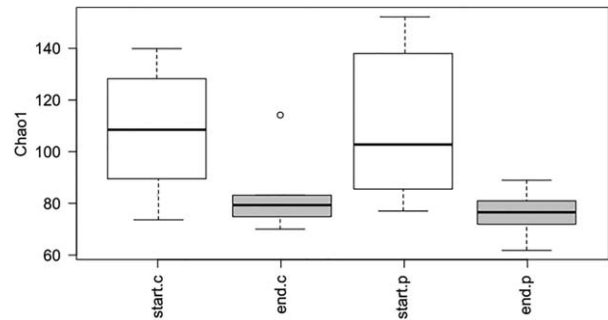


Fig. 4. Bacterial community richness (chao 1 index) at the start of the experiment (white) and the end of the experiment (grey). c = continuous ($n = 6$) and p = pulsed substrate delivery ($n = 6$).

pulses of substrate was directly related to the higher bacterial biomass under these conditions.

Bacterial community composition

In the 22 samples analysed, a total of 332,622 assembled and quality-filtered amplicon sequences were obtained, with the number of sequences per sample ranging from 11,959 to 23,608. At the end of the experiment, there was a significant difference in community composition between pulsed and continuous treatments (Permanova, $F[1,10]: 7.82$, *p*-value < 0.001, $R^2: 0.43$) (Fig. 3). The Proteobacteria phylum was dominant at the start and end of the experiment for both pulsed and continuous treatments, accounting for more than 90% of the reads and featured representatives from the alpha, beta and gamma-Proteobacteria classes. There was a ~50% reduction in the number of observed OTUs from the start to the end of the experiment (from 217 OTUs to 112). The estimated community richness (Chao1; Fig. 4) was also significantly lower by the end of the experiment compared to the start (two-way ANOVA, $F[1,22]: 8.36$, *p* < 0.008) but was not significantly different between treatments by the end of the experiment (ANOVA, $F(1,10): 0.012$, *p* = 0.914). The communities developing in the reactors were different from the natural lake inoculum. The natural community obtained from Lake Erken, featured Actinobacteria as the most abundant phylum with members of the ac1 lineage as prominent community members, while these were only present at very low abundances in the reactors (Table 1). Conversely, OTUs affiliated with the genus *Limnohabitans* (Betaproteobacteria) and *Sphingobacteria* (Alphaproteobacteria) were more abundant in the reactors while only present in low abundances in the lake inoculum (Table 1).

EdgeR was used to identify taxa that were significantly (*p* < 0.05) over-represented in the respective treatments (Table 2). Characteristic OTUs for the pulsed treatment were *Limnohabitans-A1*, *Limnohabitans-A3* and two *Sphingomonadales* while the continuously acetate-fed treatment

Table 1. Comparison of the 30 most abundant OTUs in the inoculum (A) and experiment (B).

OTU	Relative abundance (%)			Taxonomy
	Inoculum	Continuous	Pulse	
Thirty most abundant OTUs in the Lake Erken Inoculum				
13	21.41 ± 1.7	0.028 ± 0.06	0.037 ± 0.07	Actinomycetales(100)/acl-B1(100)
15	11.78 ± 4.0	0.017 ± 0.04	0.019 ± 0.04	Opitutales(100)/Opitutaceae(100)
22	5.29 ± 0.5	0.006 ± 0.02	0.008 ± 0.02	Actinomycetales(100)/acl-A6(100)
25	4.30 ± 0.3	0.008 ± 0.02	0.005 ± 0.01	Acidimicrobiales(100)/lluma-A2(100)
28	3.73 ± 0.2	0.009 ± 0.02	0.006 ± 0.02	Burkholderiales(100)/Lhab-A1(100)
31	3.50 ± 0.0	0.004 ± 0.01	0.006 ± 0.02	Methylophilales(100)/LD28(100)
44	3.27 ± 0.2	0.003 ± 0.01	0.001 ± 0.003	Actinomycetales(100)/acl-A3(100)
24	2.96 ± 0.7	0.004 ± 0.01	0.003 ± 0.01	alfVI(100)/alfVI(100)
30	2.7 ± 0.8	0.004 ± 0.01	0.003 ± 0.01	Methylococcales(29)/Methylococcaceae(29)
39	2.57 ± 0.3	0.006 ± 0.01	0.006 ± 0.01	Actinomycetales(100)/acl-C2(100)
38	2.42 ± 0.2	0.004 ± 0.01	0.003 ± 0.01	Actinomycetales(100)/acTH1-A1(100)
46	2.40 ± 0.2	0.004 ± 0.01	0.003 ± 0.01	Burkholderiales(100)/PnecB(96)
211	2.33 ± 0.2	0.003 ± 0.01	0.003 ± 0.01	Actinomycetales(100)/acl-B1(59)
400	1.92 ± 0.1	0.006 ± 0.01	0.006 ± 0.01	Actinomycetales(100)/acl-A7(100)
159	1.85 ± 0.5	0.008 ± 0.02	0.002 ± 0.01	Actinomycetales(100)/acl-A6(69)
33	1.48 ± 0.4	0.008 ± 0.01	0.003 ± 0.01	Rickettsiales(100)/LD12(100)
47	1.20 ± 0.0	0.003 ± 0.01	0.004 ± 0.01	Burkholderiales(100)/betVI(100)
35	1.18 ± 0.2	0.137 ± 0.24	0.017 ± 0.03	alfVIII(100)/alfVIII(100)
42	1.07 ± 0.1	0.001 ± 0.002	0.001 ± 0.001	Acidimicrobiales(100)/lluma-A1(100)
61	1.03 ± 0.0	0.002 ± 0.005	0.003 ± 0.01	Sphingobacteriales(100)/bacl-A1(100)
68	1.02 ± 0.0	0.001 ± 0.002	0 ± 0	Actinomycetales(100)/Luna1-A2(95)
101	0.93 ± 0.2	0.003 ± 0.007	0.001 ± 0.01	Burkholderiales(100)/betVII-B1(97)
50	0.93 ± 0.1	0.001 ± 0.005	0.001 ± 0.002	verI(100)/Xip-B1(100)
74	0.75 ± 0.1	0 ± 0	0.001 ± 0.003	Actinomycetales(100)/acl-A4(100)
80	0.68 ± 0.1	0 ± 0	0 ± 0	Burkholderiales(100)/Lhab-A4(98)
382	0.67 ± 0.1	0.005 ± 0.01	0.002 ± 0.01	Burkholderiales(100)/Lhab-A1(96)
67	0.67 ± 0.2	0.013 ± 0.046	0.001 ± 0.003	LiUU-3-334(100)/LiUU-3-334(100)
57	0.56 ± 0.0	0.001 ± 0.003	0.001 ± 0.002	Sphingobacteriales(99)/bacl-B1(42)
60	0.56 ± 0.1	0.001 ± 0.003	0 ± 0	Sphingobacteriales(100)/Algor(100)
59	0.55 ± 0.1	0 ± 0	0.001 ± 0.002	Actinomycetales(39)/acSTL-A2(19)
Thirty most abundant OTUs in the Experimental reactors				
1	0.09 ± 0.05	9.94 ± 6.14	23.0 ± 6.17	Burkholderiales(100)—Lhab-A1(51)
0	0.18 ± 0.14	16.87 ± 16.08	13.8 ± 11.7	Sphingomonadales(100)—Sphingo(97)
5	0.02 ± 0.01	13.61 ± 16.12	7.1 ± 10.38	Pseudomonadales(100)—Pseudo-A1(100)
2	0.06 ± 0.03	8.70 ± 7.65	8.1 ± 6.11	Rhizobiales(87)—alfI-B2(44)
3	0.03 ± 0.04	11.77 ± 9.74	2.7 ± 2.3	Burkholderiales(100)—Lhab-A3(49)
268	0.02 ± 0.03	1.51 ± 1.42	9.2 ± 8.92	Sphingomonadales(100)—Sphingo(100)
4	0 ± 0	4.85 ± 4.01	4.9 ± 3.62	Methylophilales(90)—LD28(73)
14	0.11 ± 0.01	3.21 ± 2.37	4.0 ± 2.66	Burkholderiales(100)—Lhab-A2(56)
41	0.01 ± 0.02	4.36 ± 4.07	2.7 ± 3.95	Sphingomonadales(100)—Sphingo(63)
11	0 ± 0	1.83 ± 1.04	4.8 ± 8.51	Burkholderiales(100)—Lhab-A4(79)
9	0.02 ± 0.01	2.46 ± 2.12	2.7 ± 2.9	Sphingobacteriales(100)—bacl-A2(93)
7	0.01 ± 0.02	2.26 ± 1.51	2.8 ± 2.9	Caulobacteriales(84)—Brev(75)
102	0.02 ± 0.01	4.16 ± 8.4	0.8 ± 0.86	Pseudomonadales(100)—Pseudo-A1(100)
36	0.02 ± 0.02	0.99 ± 0.95	1.6 ± 1.56	Rhizobiales(83)—alfI-B2(49)
18	0.01 ± 0.01	0.30 ± 0.45	1.7 ± 4.8	Burkholderiales(100)—Lhab-A3(89)
26	0.03 ± 0.02	0.42 ± 0.25	1.41 ± 2.0	Burkholderiales(100)—Lhab-A3(23)
117	0 ± 0	1.05 ± 1.18	0.8 ± 0.8	Sphingomonadales(100)—Sphingo(75)
17	0.02 ± 0.01	1.23 ± 2.35	0.2 ± 0.32	Pseudomonadales(100)—Acin(100)
16	0.01 ± 0.01	1.00 ± 0.81	0.42 ± 0.21	Sphingobacteriales(100)—bacl-A1(73)
148	0 ± 0	0.74 ± 0.84	0.4 ± 0.52	Sphingomonadales(63)—M-L-85(34)
19	0 ± 0	1.01 ± 2.05	0.1 ± 0.13	Pseudomonadales(100)—Acin(100)
104	0 ± 0	0.44 ± 0.55	0.5 ± 0.64	Burkholderiales(100)—Lhab-A4(39)
71	0 ± 0	0.58 ± 0.88	0.3 ± 0.26	Sphingomonadales(100)—Novo-A1(55)
20	0.01 ± 0.01	0.57 ± 0.52	0.2 ± 0.16	Caulobacteriales(100)—Brev(100)
23	0 ± 0	0.74 ± 1.47	0.01 ± 0.09	Burkholderiales(85)—PnecB(65)
6	0.01 ± 0.01	0.58 ± 0.77	0.2 ± 0.11	Sphingobacteriales(100)—Pedo(79)

Table 1. cont.

OTU	Relative abundance (%)			Taxonomy
	Inoculum	Continuous	Pulse	
380	0 ± 0	0.35 ± 0.38	0.3 ± 0.41	Sphingobacteriales(98)—bacl-A2(93)
27	0 ± 0	0.19 ± 0.17	0.2 ± 0.35	alfVI(47)—alfVI(47)
21	0.01 ± 0.01	0.21 ± 0.24	0.2 ± 0.26	Sphingobacteriales(100)—Pedo(95)
29	0 ± 0	0.33 ± 0.7	0.1 ± 0.07	Rhizobiales(95)—alfI-B1(52)

Relative abundance and standard deviation of the OTUs are shown separately for 'Inoculum', 'Continuous' and 'Pulse' samples. The relative abundances are based on read counts at the start and end of the experiment. Taxonomy contains the order and the lowest confident assignment of each OTU, subsequent values are the confidence strength of the annotation. Taxonomic affiliations are given according to the framework in Newton *et al.* (2011).

were characterized by other *Sphingomonadales* and *Limnohabitans-A3* OTUs, *Polynucleobacter (PnecB)* and *Acinetobacter (gamIII)* (Table 2). For the pulsed treatment, the indicator OTUs contributed with on average 36% of the reads at the end of the experiment, while the corresponding average for the continuous treatment was 12%.

Discussion

Substrate heterogeneity can be observed across both spatial and temporal scales in aquatic environments. Here, we measured the importance of substrate patchiness over time as a potential controlling factor for total bacterial growth yield and substrate uptake rates. All reactors received the same total amount of carbon substrates during the course of the experiment and these substrates were efficiently used up in both treatments as seen from the equally low background levels in the two treatments. Nevertheless, estimated bacterial biomass was more than twice as high in the pulsed compared to the continuous treatment (Fig. 1) and hence we argue that pulsed substrate delivery allowed for a higher proportion of the metabolically mobilized energy to be diverted to biomass production (Lennon and Cottingham, 2008) rather than being used for cellular maintenance. The difference between treatments may quite likely be due to the higher

energetic costs for taking up substrates at constantly low concentrations typical for the continuous treatment (Egli, 2010). The variable concentrations in the pulsed treatment would, in contrast, allow for less energetically expensive transport or even passive diffusion into the cell (Weiss *et al.*, 1991). We further speculate that the pulsed substrate delivery mode may foster heterotrophic communities capable of rapid transitions between physiological states, i.e. switching from growth to an inactive state (Konopka, 2000). Such a lifestyle may also enable more efficient use of resources, as cellular maintenance costs would be lower during periods of inactivity.

In contrast to our initial expectations, differences in diversity *sensu* richness did not explain the functional differences observed, since richness did not differ between treatments (Fig. 3). However, differences in estimated bacterial growth yield coincided with changes in community composition between the two treatments. Such a coupling of yield with composition has also been observed in experiments along substrate concentration gradients in batch cultures (Eiler *et al.* 2003), suggesting a coupling between community composition and substrate processing capabilities in response to availability of resources. Underlying the differences in community composition, certain OTUs were identified as being significantly overrepresented in each of the two treatments. For instance one of the representatives

Table 2. Comparison of tagwise dispersion (edgeR, R package) analysis of indicator OTUs for the respective pulsed and continuous substrate delivery treatment determined at the end of the experiment.

Taxonomical assignment	Treatment %	logFC	p-value	FDR	Treatment
α -proteobacteria (<i>Sphingo</i>)	11.59 ± 11.77	4.82	1.32E-10	1.04E-08	pulse
β -proteobacteria (<i>Lhab-A1</i>)	24 ± 5.2	2.76	1.14 E-06	4.51 E-05	pulse
α -proteobacteria (<i>Sphingo</i>)	0.4 ± 0.18	3.72	4.71 E-05	1.24 E-03	pulse
α -proteobacteria (<i>Sphingo</i>)	0.48 ± 0.33	-3.55	1.75 E-04	3.47 E-03	cont.
β -proteobacteria (<i>Lhab-A3</i>)	10.18 ± 8.89	-2.6	1.04 E-03	1.41 E-02	cont.
β -proteobacteria (<i>PnecB</i>)	0.57 ± 1.29	-4.38	1.07 E-03	1.41 E-02	cont.
β -proteobacteria (<i>Lhab-A3</i>)	0.1 ± 0.16	4.37	1.38 E-03	1.55 E-02	pulse
γ -proteobacteria (<i>gamIII</i>)	1.14 ± 2.4	-3.54	1.84 E-03	1.85 E-02	cont.

The average relative abundance for the indicated treatment is presented ± standard deviation. LogFC denote the log₂-fold change between continuous and pulsed treatments in OTU relative abundance. Taxonomic affiliations are given according to the framework presented in Newton *et al.* (2011).

of the pulsed treatment was identified as *Limnohabitans-A1* known for having an adaptive generalist life strategy and being capable of opportunistic fast growth (Jezbera *et al.*, 2013).

For the continuous treatment, the abundant and widespread planktonic freshwater lineage *Polynucleobacter* (PnecB) was significantly overrepresented (Table 2). Members of this lineage have previously been implicated in passively using acetate and other low molecular weight photoproducts in humic lakes (Hahn *et al.* 2012). Furthermore, populations equally present in the two treatments may also display functional plasticity (Agrawal, 2001), manifested as different physiological and metabolic features under the two different substrate delivery conditions. This could at least partly explain the observed differences in estimated bacterial growth yield. Since we did not directly manipulate community composition, our experimental design does not enable us to explicitly investigate the causal effects of community changes on community uptake characteristics.

While the use of highly controlled continuous flow reactors fed with a defined artificial lake water medium enabled us to isolate the effects of substrate patchiness on bacterial communities, the approach is not without limitations. For instance the removal of grazers may enrich for active bacteria that are otherwise selectively consumed and therefore rare in a natural environment (e.g., Salcher 2014). Further, the use of an artificial defined media is likely to select for a certain subset of the total lake community and this is in agreement with reactors hosting communities with lower richness as compared to the natural lake inoculum. While this prevents us from directly extrapolating our findings to lake ecosystems where also predation and other loss factors are important, our findings emphasize the potential of substrate patchiness as an important factor influencing bacterial growth yield and consequently also the fate of organic substrates processed by heterotrophs. Another factor that may influence the communities is potential biofilm development in the reactors. While no such biofilms were visibly observed at the end of the extended incubation, we cannot exclude the possibility that a lesser number of bacteria with such a lifestyle could have contributed to substrate use in the reactors. Regardless of these limitations, the flow-through reactor design allowed us to study bacterioplankton responses to the heterogeneity of substrates, a feature known to be prominent in natural ecosystems.

Episodic events such as massive algal blooms and spring floods flushing in substrates from the watershed can shape concentrations of organic matter substrates over larger scales (Kaplan and Bott, 1989; Bertilsson and Jones, 2003; Raymond *et al.*, 2016). More frequent but less dramatic events such as wind-driven sediment resuspension and photochemical production of acetate and related photoproducts in sunlit surface waters may create intermediate-scale

heterogeneity in organic substrates (Bertilsson and Tranvik, 1998). Microscale patchiness has received less attention and is less evident, but substrate release-plumes from degrading organic particles suspended in the water or short-lived pulses of dissolved organic substrates from a phytoplankton cell lysed by a virus or the organic compounds released by bacterivore sloppy feeding, will create substantial microscopic-scale heterogeneity that may influence local substrate availability (Stocker, 2012). Considering these contrasting spatial and temporal scales and the widespread occurrence of processes creating substrate heterogeneity, our observation of substantial differences in estimated bacterial growth yield and the linked differences in diversion of dissolved organic matter into biomass and the food web merits further study.

Experimental procedures

Inoculum and artificial lake water

Surface water for the experiment was collected from Lake Erken, situated in central Sweden (59.83°N, 18.64°W) on 23 of April 2014. To remove grazers, water was first vacuum filtered (3.5 psi lb/in²) through 0.7 µm glass fiber filters (Whatman™, grade GF/F) that had been combusted at 450°C for 4 h. The recovered bacterial community in the filtrate was stored in the dark at 20°C for a week under batch growth in a 1 L bottle (Schott, Duran) to allow the bacterial community to stabilize to *in vitro* conditions. Cell abundance was subsequently determined and 2.1×10^6 cells were added to a batch-incubation with 100 mL artificial lake media (Supporting Information Table S1; Bastviken *et al.*, 2004), to obtain a natural bacterial inoculum adapted to the artificial lake water media and the acetate carbon source. Some of the media components were autoclaved separately to avoid precipitation (KHCO₃, Na₂HPO₄, sodium acetate and micro constituents). Sodium acetate was added to the media to a final concentration of 220 µg C L⁻¹ (Supporting Information Table S1).

Evolving continuous cultures

At first, twelve replicate continuous cultures were established in sterile 200 mL glass cylinder reactors. Each reactor was inoculated with 4.5×10^4 cells, from the batch culture described above. Two 5-L bottles with media were connected to six incubation reactors each. Long glass tubes connected to silicone tubes directed the media from the reservoir to the peristaltic pump and from the pump to the incubation bottle. Each incubation bottle was sealed with a Teflon-coated membrane with holes to fit a stainless steel needle for sampling and through which addition of acetate pulses were made during the experiment. An air filter was also connected through the membrane seal with a silicone tube to avoid pressure build-up inside the reactors. Reactors were constantly stirred with magnetic rods. These reactors were maintained for a month at 18°C in the dark, while aseptically and continuously feeding them with sterile artificial lake water media and sodium acetate. Each reactor received a total of 21 µg C day⁻¹ using a peristaltic pump (ISMATEC, Switzerland) at a

continuous flow rate of 4 mL h^{-1} (hydrological turnover time 2.1 days). After one month of continuous pre-cultivation, the contents in the 12 reactors were pooled, mixed and aseptically redistributed to 12 new reactors. This was considered the start of the experimental incubation, where the reactors were exposed to two different treatments. Six reactors were maintained under a sustained continuous substrate delivery regime ($21 \mu\text{g C day}^{-1}$) while the six remaining reactors were continuously fed artificial lake water medium devoid of acetate at identical flow rates and an equal total amount of acetate as for the continuous reactors was provided as a substrate spike every second day, using a syringe to aseptically add 1.4 mL from a 29 mg C L^{-1} acetate stock.

Bacterial cell abundance was measured daily during the one month-long experiment while bacterial cells for DNA-based community analyses were collected at the start and end of the experimental incubations.

Acetate degradation and uptake

At the end of the experimental incubation, we evaluated acetate uptake capacity in both pulsed and continuously acetate-fed reactors by spiking all incubation reactors with an identical (high) amount of acetate ($220 \mu\text{g C L}^{-1}$) and then tracking the substrate using HPLC-based analyses of organic acids. Samples were collected from each reactor prior to the addition of acetate to determine the background acetate concentration. Later, concentrations were measured every second hour during a 12-h period. For each time point, 1 mL of water was collected in polypropylene micro-centrifugation tubes (Eppendorf) that had been thoroughly rinsed with pure water (Milli-Q Advantage A 10 ultrapure water purification system). Samples were filtered through pre-rinsed $0.2 \mu\text{m}$ pore size Supor 200 filters (Pall Corporation, Port Washington, NY, USA). In parallel, Milli-Q water blanks were processed in the same way to account for acetate contamination from the handling. A Varian ProStar HPLC system featuring a model 430 auto-sampler with a $100 \mu\text{L}$ loop and two model 210 pumps with titanium pump heads, a Thermo Scientific Dionex RFC-30 Reagent Free Controller (with a EGC III KOH cartridge), an AERS 500 suppressor (operated in external water mode) as well as a Dionex ED40 conductivity detector was used for this purpose. Separations were performed at a flow rate of 1.5 mL min^{-1} on a Thermo Scientific Dionex IonPac AS11-HC column ($4 \times 250 \text{ mm}$) with an IonPac AG11-HC guard column ($4 \times 50 \text{ mm}$) using a hydroxide gradient (1 mM 0 to 15 min, 1 mM to 50 mM 15 to 20 min, hold for 5 min, 50 mM to 1 mM and hold for 5 min). To compare acetate uptake between treatments, acetate degradation rates during the first 6 h following substrate addition were estimated using linear regression.

In parallel, cellular uptake of acetate was evaluated at lower concentrations with tracer additions of ^{14}C labelled acetate (Perkin Elmer, Acetic Acid, Sodium salt [$1\text{-}^{14}\text{C}$], 37 MBq). From each incubation reactor, triplicate 5 mL aliquots were sampled and transferred to pre-rinsed 15 mL polypropylene screwcap tubes (Falcon), each replicate was amended with ^{14}C -acetate diluted (1:5) with non-labelled acetate to a final concentration of $17.3 \mu\text{g C L}^{-1}$. One of the replicates served as sterile control with formaldehyde added prior to the radio-tracer addition (final concentration 2%). The samples were then incubated in darkness for 0.5 h. Incubations were

terminated by adding formaldehyde, as was done in controls. Samples were filtered through $0.22 \mu\text{m}$ pore-size membrane filters (GSWP, MF-Millipore), pre-soaked in sodium acetate (1 mg L^{-1}) prior to use in order to minimize surface absorption of ^{14}C labelled substrate to the filter. Filtrations were carried out in a 12-position vacuum filtration manifold that was thoroughly rinsed in between samples. Filters, with the cell side facing up, were placed in scintillation vials and covered with scintillation cocktail (5 mL filter count, LSC cocktail, Perkin Elmer) and swirled gently. After 10 h, the radioactivity in each sample was measured by liquid scintillation with a Beckman LS 1801 scintillation counter (as previously described by Bertilsson *et al.*, 2007). Decays per minute (DPM) were calculated using quench correction and uptake rates were reported after correcting for incubation time and volume. For both radiotracer- and HPLC-based acetate uptake estimates, total rates were also normalized for differences in cell abundances and were reported as cell specific uptake rates.

Bacterial community composition and diversity

To collect bacterial cells, a total of 10 mL of water was collected from each reactor by vacuum filtration through $0.2 \mu\text{m}$ Supor 200 filters (Pall Corporation, Port Washington, NY, USA). Filters were stored at -80°C until DNA extraction was performed using the Power Soil DNA isolation kit as recommended by the manufacturer (MoBio Laboratories, Carlsbad, CA, USA). Each sample was initially amplified in duplicate using bacterial primer constructs targeting the variable V4 region (amplification method in Supporting Information Tables S2 and S3). Duplicates were pooled and purified using the Agencourt AMPure (Beckman Coulter) as recommended by the manufacturer, and then used as template in a second PCR step (method in Supporting Information Tables S4 and S5) in order to attach standard Illumina handles and index/barcode primers (primer and barcode sequences in Supporting Information Table S6). PCR products were purified as mentioned above, and quantified by fluorescence using the PicoGreen assay (Quant-iT PicoGreen, Invitrogen). The individual barcoded amplicon samples were pooled in equimolar amounts for sequencing at the SciLifeLab SNP/SEQ next generation sequencing facility (hosted by Uppsala University) on an Illumina MiSeq platform using $2 \times 300 \text{ bp}$ chemistry.

The raw amplicon sequencing data was demultiplexed and sequence-pairs were assembled using an in-house bioinformatic pipeline described in Sinclair *et al.* (2015). The pipeline further removed sequences with missing primers and unassigned base pairs. The quality-filtered and assembled reads were clustered into operational taxonomical units (OTUs) using UPARSE (3% sequence dissimilarity cutoff; Edgar, 2013). Taxonomy was assigned using CREST (Lanzén *et al.*, 2012) and the SilvaMod ribosomal database as well as the Naive Bayesian Classifier (Wang *et al.*, 2007) in combination with a freshwater specific 16S rRNA gene database (Newton *et al.*, 2011). Raw sequences were deposited in the GenBank sequence read archive (SRA) under accession number SRP075169. Statistical analyses of bacterial community composition between treatments were performed using R software (R Core Team 2014). Prior to analysis, samples were randomly downsized to the sample with the least number of reads (11,959 reads).

Bacterial abundance and biomass

Bacterial cell abundance was analysed by flow cytometry after cells had been fixed with formaldehyde (final concentration 2%) and stained with the fluorescent dye Syto13 (Molecular probes, Invitrogen, Carlsbad, CA, USA) according to del Giorgio *et al.* (1996). Cell counting was performed with a flow cytometer equipped with a 488 nm blue solid state laser (Cyflow Space, Partec, Görlitz, Germany). A volume of 50 μ l was counted and green fluorescence was used as trigger during the measurement. The flow cytometry counts were analysed using Flowing Software version 2.5 (Perttu Terho, Centre for Biotechnology, Turku Finland). Median forward scatter was used as a proxy for average bacterial cell size and biomass in individual cell samples (Bertilsson *et al.*, 2003). Without additional calibration, this metric does not provide information on absolute cell size, but can detect differences in this cellular property between samples and treatments. Analysis of forward scatter results showed that cell size was not significantly different between the treatments and cell counts were therefore used to compare bacterial growth yield between continuous and pulsed reactors.

Data analysis

Differences in cell abundance and cell size between treatments were determined with a repeated measures ANOVA (within-subjects ANOVA, AOV function, R software). Cell size measures were compared between the treatments for day 19 of the incubation ($n=6$ for each treatment). Differences in community-level acetate uptake rates from HPLC and ^{14}C tracer experiments were analysed with student's t-test both before and after normalizing for cell abundance differences between treatments.

Differences in bacterial community composition between treatments were visualized in a non-metric multidimensional scaling plot (metaMDS function, package ggplot2, Wickham, 2009) using Bray-Curtis dissimilarity index. Significant differences were tested with a one-way permutational ($n=999$) manova (adonis function, vegan package, Oksanen *et al.*, 2015).

Alpha diversity was described with the Chao1 index of species richness. Significant differences in diversity between start and end of the experiment as well as between the two treatments at the end of the experiment were tested with a two-way ANOVA.

In order to see how many OTUs that were significantly over-represented in the respective treatment (pulse versus continuous), we estimated the dispersion of our data to take into account outlier-driven bias. All OTUs were ranked according to their association to each treatment and the tagwise dispersion function (edgeR, R package) ranked the OTUs according to their coefficient of variation between replicates. The OTUs that were significantly different between the treatments (p -value < 0.05) were retrieved. In order to adjust the p -value using a false discovery rate (FDR) the TopTag function was applied.

Acknowledgements

We thank Lars Tranvik and Hannes Peter for providing the chemostat reactors and technical assistance to run them.

We further thank Christoffer Bergvall for HPLC measurements. Pilar L. Hernandez for amplification and barcoding work and anonymous reviewers for constructive feedback on the manuscript. We also thank the Uppsala Multidisciplinary Center for Advanced Computational Science (UPPMAX) for providing data storage resources. We thank the SciLifeLab SNP/SEQ facility hosted by Uppsala University for the Illumina Miseq sequencing. The study was funded by the Vetenskapsrådet Swedish Research Council (grant 2012–3892 to S.B.)

References

- Agrawal, A.A. (2001) Phenotypic plasticity in the interactions and evolution of species. *Science* **294**: 321–327.
- Bastviken, D., Persson, L., Odham, G., and Tranvik, L.J. (2004) Degradation of dissolved organic matter in oxic and anoxic lake water. *Limnol Oceanogr* **49**: 109–116.
- Beier, S., and Bertilsson, S. (2011) Uncoupling of chitinase activity and uptake of hydrolysis products in freshwater bacterioplankton. *Limnol Oceanogr* **56**: 1179–1188.
- Bertilsson, S., and Tranvik, L.J. (1998) Photochemically produced carboxylic acids as substrates for freshwater bacterioplankton. *Limnol Oceanogr* **43**: 885–895.
- Bertilsson, S., and Jones, J.B. (2003). Supply of dissolved organic matter to aquatic ecosystems: autochthonous sources. In *Aquatic Ecosystems: Interactivity of Dissolved Organic Matter*. Findlay, S.E.G., Sinsabaugh, R.L. (eds). San Diego: Academic Press/Elsevier Science, pp. 3–24.
- Bertilsson, S., Berglund, O., Karl, D.M., and Chisholm, S.W. (2003) Elemental composition of marine *Prochlorococcus* and *Synechococcus*: Implications for the ecological stoichiometry of the sea. *Limnol Oceanogr* **48**: 1721–1731.
- Bertilsson, S., Eiler, A., Nordqvist, A., and Jørgensen, N.O.G. (2007) Links between bacterial production, amino-acid utilization and community composition in productive lakes. *ISME J* **1**: 532–544.
- Blackburn, N., Fenchel, T., and Mitchell, J. (1998) Microscale nutrient patches in planktonic habitats shown by chemotactic bacteria. *Science* **282**: 2254–2256.
- Carrero-Colón, M., Nakatsu, C.H., and Konopka, A. (2006) Microbial community dynamics in nutrient-pulsed chemostats. *Microb Ecol FEMS* **57**: 1–8.
- Edgar, R.C. (2013) UPARSE: highly accurate OTU sequences from microbial amplicon reads. *Nat Methods* **10**: 996–998.
- Egli, T. (2010) How to live at very low substrate concentration. *Water Res* **44**: 4826–4837.
- Eichinger, M., Kooijman, S.A.L.M., Sempéré, R., Lefèvre, D., Grégori, G., Charrière, B., and Poggiale, J.C. (2009) and release of dissolved organic carbon by marine bacteria in a pulsed-substrate environment: from experiments to modelling. *Aquat Microb Ecol* **56**: 41–54.
- Eiler, A., Langenheder, S., Bertilsson, S., and Tranvik, L.J. (2003) Heterotrophic bacterial growth efficiency and community structure at different natural organic carbon concentrations. *Appl Environ Microbiol* **69**: 3701–3709.
- van Gernerden, H. (1974) Coexistence of organisms competing for the same substrate: An example among the purple sulfur bacteria. *Microb Ecol* **1**: 104–119.
- del Giorgio, P.A., and Cole, J.J. (1998) Bacterial growth efficiency in natural aquatic systems. *Annu Rev Ecol Syst* **29**: 503–541.

- del Giorgio, P.A., Bird, D., Prairie, Y., and Planas, D. (1996) Flow cytometric determination of bacterial abundance in lake plankton with green nucleic acid stain SYTO 13. *Limnol Oceanogr* **41**: 783–789.
- Grover, J.P., and Chrzanowski, T.H. (2000) Seasonal patterns of substrate utilization by bacterioplankton: case studies in four temperate lakes of different latitudes. *Aquat Microb Ecol* **23**: 41–54.
- Hahn, M.W., Scheuerl, T., Jezberová, J., Koll, U., Jezbera, J., Šimek, K., et al. (2012) The passive yet successful way of planktonic life: genomic and experimental analysis of the ecology of a free-living Polynucleobacter population. *PLoS One* **7**: e32772.
- Hutchinson, A.G.E. (1961) The paradox of the plankton. *Am Nat* **95**: 137–145.
- Jezbera, J., Jezberová, J., Kasalický, V., Šimek, K., Hahn, M.W., and Badger, J.H. (2013) Patterns of limnohabitans microdiversity across a large set of freshwater habitats as revealed by reverse line blot hybridization. *PLoS One* **8**: e58527.
- Judd, K.E., Crump, B.C., and Kling, G.W. (2006) Variation in dissolved organic matter controls bacterial production and community composition. *Ecology* **87**: 2068–2079.
- Kaplan, L.A., and Bott, T.L. (1989) Diel fluctuations in bacterial activity on streambed substrata during vernal algal blooms: Effects of temperature, water chemistry, and habitat. *Limnol Oceanogr* **34**: 718–733.
- Konopka, A. (2000) Theoretical analysis of the starvation response under substrate pulses. *Microb Ecol* **38**: 321–329.
- Konopka, A., Zakharaova, T., and Nakatsu, C. (2002) Effect of starvation length upon microbial activity in a biomass recycle reactor. *J Ind Microbiol Biotechnol* **29**: 286–291.
- Konopka, A., Carrero-Colón, M., and Nakatsu, C.H. (2007) Community dynamics and heterogeneities in mixed bacterial communities subjected to nutrient periodicities. *Environ Microbiol* **9**: 1584–1590.
- Landa, M., Cottrell, M.T., Kirchman, D.L., Kaiser, K., Medeiros, P.M., Tremblay, L., et al. (2014) Phylogenetic and structural response of heterotrophic bacteria to dissolved organic matter of different chemical composition in a continuous culture study. *Environ Microbiol* **16**: 1668–1681.
- Langenheder, S., Lindström, E.S., and Tranvik, L.J. (2005) Weak coupling between community composition and functioning of aquatic bacteria. *Limnol Oceanogr* **50**: 957–967.
- Lanzén, A., Jørgensen, S.L., Huson, D.H., Gorfer, M., Grindhaug, S.H., Jonassen, I., et al. (2012) CREST—classification resources for environmental sequence tags. *PLoS One* **7**: e49334.
- Lauro, F.M., McDougald, D., Thomas, T., Williams, T.J., Egan, S., Rice, S., et al. (2009) The genomic basis of trophic strategy in marine bacteria. *Proc Natl Acad Sci USA* **106**: 15527–15533.
- Lennon, J.T., and Cottingham, K.L. (2008) Microbial productivity in variable resource environments. *Ecology* **89**: 1001–1014.
- Lovley, D.R., and Klug, M.J. (1982) Intermediary metabolism of organic matter in the sediments of a eutrophic lake. *Appl Environ Microbiol* **43**: 552–560.
- Newton, R.J., Jones, S.E., Eiler, A.E., McMahon, K.D., and Bertilsson, S. (2011) A guide to the natural history of freshwater lake bacteria. *Microbiol. Mol Biol Rev* **75**: 14–49.
- Oksanen, J., Guillaume, B.F., Kindt, R., Legendre, P., Minchin, P.R., O'hara, R.B., et al. (2015) *vegan*: Community Ecology Package. R Package Version 2.2-1, <http://CRAN.R-project.org/package=vegan>
- Pernthaler, A., Pernthaler, J., Eilers, H., and Amann, R. (2001) Growth patterns of two marine isolates: adaptations to substrate patchiness? *Appl Environ Microbiol* **67**: 4077–4083.
- R Core Team. (2014). R Foundation for statistical computing; Vienna Austria. <http://www.R-project.org/>.
- Raymond, P.A., Saiers, J.E., and Sobczak, W.V. (2016) Hydrological and biogeochemical controls on watershed dissolved organic matter transport: Pulse-shunt concept. *Ecology* **97**: 5–16.
- Salcher, M.M. (2014) Same same but different: ecological niche partitioning of planktonic freshwater prokaryotes. *J Limnol* **73**: 74–87.
- Salcher, M.M., Pernthaler, J., and Posch, T. (2011) Seasonal bloom dynamics and ecophysiology of the freshwater sister clade of SAR11 bacteria 'that rule the waves' (LD12). *ISME J* **5**: 1242–1252.
- Salcher, M.M., Posch, T., and Pernthaler, J. (2013) In situ substrate preferences of abundant bacterioplankton populations in a prealpine freshwater lake. *ISME J* **7**: 896–907.
- Sinclair, L., Osman, O.A., Bertilsson, S., and Eiler, A. (2015) Microbial community composition and diversity via 16S rRNA gene amplicons: Evaluating the illumina platform. *PLoS One* **10**: 1–18.
- Stocker, R. (2012) Marine microbes see a sea of gradients. *Science* **338**: 628–633.
- Stocker, R., Seymour, J.R., Samadani, A., Hunt, D.E., and Polz, M.F. (2008) Rapid chemotactic response enables marine bacteria to exploit ephemeral microscale nutrient patches. *Proc Natl Acad Sci USA* **105**: 4209–4214.
- Tranvik, L.J. (1988) Availability of dissolved organic carbon for planktonic bacteria in oligotrophic lakes of differing humic content. *Microb Ecol* **16**: 311–322.
- Vallino, J.J., Hopkinson, C.S., and Hobbie, J.E. (1996) Modeling bacterial utilization of dissolved organic matter: Optimization replaces Monod growth kinetics. *Limnol Oceanogr* **41**: 1591–1609.
- Wang, Q., Garrity, G.M., Tiedje, J.M., and Cole, J.R. (2007) Naïve Bayesian classifier for rapid assignment of rRNA sequences to the new bacterial taxonomy. *Appl Environ Microbiol* **73**: 5261–5267.
- Weiss, M.S., Abele, U., Weckesser, J., Welte, W., Schiltz, E., and Schulz, G.E. (1991) Molecular architecture and electrostatic properties of a bacterial porin. *Science* **254**: 1627–1630.
- Wickham, H. (2009). *ggplot2: elegant Graphics for Data Analysis*. New York: Springer.

Supporting information

Additional Supporting Information may be found in the online version of this article at the publisher's web-site:

Fig. S1. Average forward scatter of Syto13 fluorescence labelled bacterial cells in the respective treatment and 10 day time interval. Boxes represents the 25–50 percentile range percentile with error bars representing 1.5 times the inter quantile range. Outliers are given as individual points.

Table S1. Artificial lake media modified from Bastviken et al. (2004). Some of the media components were

autoclaved separately to avoid precipitation (KHCO₃, Na₂HPO₄, sodium acetate and Micro constituents). Acetate was only supplied to the media for the continuous treatment reactors.

Table S2. Amplification method used to prepare the first PCR reaction

Table S3. Thermocycling program used in the first PCR step.

Table S4. Amplification method used to prepare the second PCR reaction.

Table S5. Thermocycling program used in the second PCR step

Table S6. Bacterial primer (Illumina adapters) sequences used in the first PCR reaction targeting the variable region V4 and Illumina handles with indexes that were attached in the second PCR step

Table S7. Acetate uptake rates in reactors at the end of the experimental incubations estimated from ¹⁴C acetate uptake during 0.5 h incubations.